SOVIET PHYSICS JETP VOLUME 11, NUMBER 3 SEPTEMBER, 1960

EQUATION OF STATE FOR ALUMINUM, COPPER, AND LEAD IN THE HIGH PRESSURE REGION

L. V. AL' TSHULER, S. B. KORMER, A. A. BAKANOVA, and R. F. TRUNIN

Submitted to JETP editor October 7, 1959

J. Exptl. Theoret. Phys. (U.S.S.R.) **38**, 790-798 (March, 1960)

An equation of state for metals is considered, which differs from the Mie-Grüneisen equation of state for a solid body in taking into account the electronic components of the energy and pressure. New data from the dynamic compression of metals are presented, on the basis of which equations of state are derived for aluminum, copper, and lead in the high pressure region.

INTRODUCTION

THE behavior of metals under pressures of several million atmospheres and temperatures of some tens of thousands of degrees may be described by an equation of state, if their compressibility curves at the absolute zero of temperature, the specific heats of the lattice and the electron gas, and their Grüneisen coefficients (defined as the ratio of the thermal pressure to the thermal energy density) are known. Such equations of state cannot be obtained theoretically, since quantum-statistical calculations of the compressibility by the Thomas-Fermi and Thomas-Fermi-Dirac methods lead to an increased pressure which does not reduce to zero at normal density. Solid state theory also does not allow the calculation of Grüneisen coefficients for the lattice, establishing merely the connection between these coefficients and the extrapolated "cold" compression curve.[1-3] For the non-transition metals, our knowledge of the thermal components of energy and pressure caused by the excitation of the electron gas is quite complete and reliable. The validity of the theoretical results in this field are confirmed by measurements of the electronic specific heat at temperatures close to absolute zero. At the present time, of course, we can deal only with semi-empirical equations of state, based on direct experimental measurements of the compressibility.

As a source of information about the pressure region of interest to us, the authors have made use of data from individual single dynamic compressions. The transition from a dynamic adiabatic to the general equation of state connecting the pressure with the density and temperature is possible if additional data is available, for example on the shock compressibility of porous bodies,[4] or with the aid of the theoretical relationships, mentioned above, between the Grüneisen coefficients and the curve of cold compression. This second method has been put into practice in a work by Walsh and his collaborators,[5] devoted to the state equations for metals up to pressures of 5×10^5 atm.

The main difference between our work and the above consists in the considerably wider range of pressures and temperatures covered, and in taking into account the electronic components of energy and pressure, which cannot in any case be neglected for temperatures of 1 — 2 ev. In this paper we also present data on the dynamic compression of aluminum up to pressures of 2×10^6 atm and the results of new measurements of the compressibility of copper, lead, and iron at pressures of 10^6, 2×10^6, and 4×10^6 atm.

1. DYNAMIC ADIABATS OF ALUMINUM, COPPER, LEAD, AND IRON

The dynamic adiabats of copper and lead up to 5×10^5 atm have been described by Walsh[5] and in reference 6. In the present paper we also present the results of dynamic compression measurements on these metals up to pressures of 3.5×10^6 atm. For aluminum the observed range of pressures has amounted to 5×10^5 atm.[5,7,8] In this section we present the results of the compression of aluminum by strong shock waves up to 2×10^6 atm, obtained in the authors' laboratory, and new results on copper, lead, and iron in the pressure range from 10^6 to 4×10^6 atm. To improve the precision, it was necessary to make new measurements for the following reason. The dynamic adiabat for iron, used in reference 6 as a reference standard for determining the compressibilities of other elements at 1.3

TABLE I

Serial No.	Striker material	Striker speed, km/sec	D, km/sec	U, km/sec	P, 10^{10} d/cm²	ρ/ρ_0	D, km/sec	U, km/sec	P, 10^{10} d/cm²	ρ/ρ_σ
					Aluminum				Copper	
I	Aluminum	5.60	9.13	2.80	69.3	1.442	6.64	1.82	107.9	1.377
II	Iron	5.60	10.39	3.70	104.2	1.553	8.06	2.71	195.0	1.506
III	Iron	9.10	—	—	—	—	10.58	4.43	418.7	1.720
IV	Iron	8.64	12.94	5.62	197,1	1.767	10.12	4.14	374.0	1.692
					Lead				Iron	
I	Aluminum	5.60	4.92	1.88	104.9	1,618	7.01	1.90	104,5	1.372
II	Iron	5.60	6.07	2.76	190.0	1,834	8.44	2.80	185.5	1.496
III	Iron	9.10	8.26	4.45	417.0	2,168	11.26	4.55	402.2	1,678
IV	Iron	8.64	7.74	4.18	366.9	2,174	10,67	4.26	356.8	1,664

$\times 10^6$ atm, was obtained in reference 4 by the "splitting-off" method, i.e., by a comparison of the shock wave velocity in an iron plate with the speed W of expansion of the rear surface of the plate after the passage of the shock wave through it. The material velocity in this case was taken to be approximately $\frac{1}{2}$W, since the calculated corrections for the failure of the rûle of doubled material velocity were small. The actual error due to violation of the doubling rule could have been larger. Accordingly, new measurements of the dynamic compressibility of iron, lead, and copper in this region have been carried out by the deceleration method,[4] by recording the speed of a shock wave in the receiver and the speed of a plate, smoothly accelerated by explosion products, which strikes the receiver.

Another reason for possible inaccuracies in the previous measurements arises from the decay of the shock wave in the material of the screen which protects the sample, and in the sample itself. In order to exclude this error, the new experiments were carried out with thin screens, using a short base-line of 3 to 4 mm for the measurements. Both these effects lead to errors of the same sign, increasing the degree of compression. The suggestion that the adiabat may have a "stiffer" slope in the region of 2×10^6 atm pressure has also been expressed by Walsh (private communication).

In the first group of experiments, the pressure was created by the impact of an aluminum plate 2 mm thick and 70 mm in diameter.* After being put in place on the explosive charge, the plate was surrounded by a steel ring 120 mm in diameter and of the same thickness. The higher pressure of the explosion products caused by reflection of the detonation wave from the surface of the steel ring prevented the edges of the plate from lagging behind. In the second group of experiments the striker was a steel disk 1.5 mm thick and 70 mm in diameter, driven by the products of an explosion inside a massive lead cylinder, 90 mm thick, to a speed of 5.6 km/sec. By this means, pressures close to 2×10^6 atm were attained in iron, copper, and lead (185.5×10^{10}, 195.0×10^{10}, and 190.0×10^{10} d/cm²). Pressures of 4×10^6 atm were obtained with steel striker speeds of 9.1 km/sec. The heating of the aluminum and steel strikers during the driving process was approximately equal in all runs, and it is estimated that it did not exceed a few hundred degrees. In the first two groups of experiments the screens were made of the same material as the test samples; in the third group it was made of the same material as the striker.

The striker speed, the results of the wave-velocity measurements in the test piece, and the parameters obtained for the points by graphical constructions on the pressure-velocity diagrams are shown in Table I. The following notation has been used in the table: D is the wave velocity, U the material velocity behind the shock wave front, P the pressure, ρ the density behind the wave front, ρ_0 the density of the initial state ahead of the front, and $\sigma = \rho/\rho_0$ is the relative compression. Each value in the table was obtained as the mean of the values from 4 to 6 experiments. In each run the time recording was carried out on three double-beam oscilloscopes. The inaccuracy in the determination of the quantities D and W did not exceed 1%.

In Group IV of the table are shown the parameters of the shock waves in copper, lead, and iron obtained for a striker velocity of 8.64 km/sec, taken from reference 6. The slight changes in the

---

*The possibility of obtaining high pressures by impact of a plate driven by explosion products was indicated in 1948 by E. I. Zababakhin. Using this method, Yu. F. Alekseev measured in 1949 the compressibility of aluminum up to pressures of 500,000 atm.

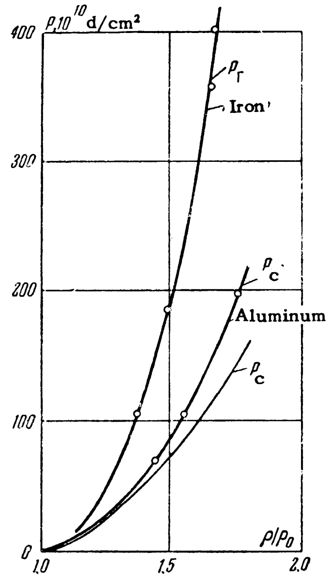

FIG. 1. Shock adiabats for iron and aluminum, and the curve of cold compression for aluminum.

parameters as compared with reference 6 are due to the introduction of the corrections to allow for the decay of the shock wave in the screen and the sample. New data have also been included on the compressibility of aluminum at pressures close to 2×10^6 atm (197.1×10^{10} d/cm^2).

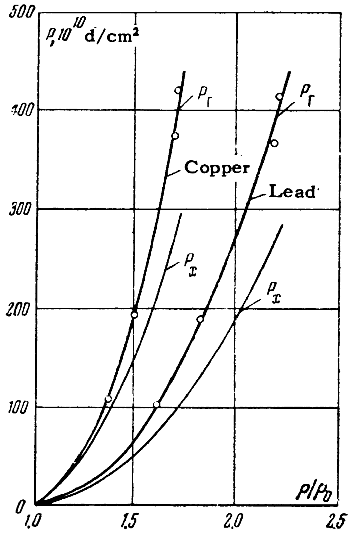

FIG. 2. Shock adiabats and curves of cold compression for copper and lead.

The points on the shock adiabat thus obtained are shown in Figs. 1 and 2. The thick lines in the figures represent the positions of the adiabats constructed from the data in the present paper. By comparison with references 4 and 6, the greatest change is in the position of the lead adiabat, which has been shifted to the left, in the direction of lower σ, by 3 to 5%. For copper and iron the changes are small.

Analytical expressions for the dynamic adiabats in the form

$$P_\Gamma = \Sigma a_k (\sigma - 1)^k \qquad (1)$$

contain the coefficients a_k, the first three of which are determined by the parameters of the material under normal conditions in the case of copper, aluminum, and lead, as will be shown below. The dynamic adiabat for iron in the pressure range from 5×10^5 to 5×10^6 atm is described by five coefficients. There is no connection between these coefficients and the parameters for iron under normal conditions, since, according to Bancroft,[9] a phase transition occurs in iron at a pressure of 1.3×10^5 atm. The coefficients a_k are shown in Table II. The relationships between the wave and material velocities is given in Table III. For the values of P_Γ as a function of σ, see Tables V to VII below.

TABLE II

k	Values of a_k, 10^{10} d/cm^2			
	Aluminum	Copper	Lead	Iron
1	73.1	137.0	41.4	30.3
2	152.7	271.7	101.7	724.5
3	143.5	224.0	120.0	—271.2
4	—887	1078	—43	—14
5	2862	—2967	547	852
6	—3192	3674	—801	—
7	1183	—1346	312	—

2. THE FORM OF THE EQUATIONS OF STATE

We shall write the equation of state and the expression for the internal energy in the additive form

$$P = P_c + P_{\text{t.l.}} + P_{\text{t.e.}}, \quad E = E_c + E_{\text{t.l.}} + E_{\text{t.e.}} \qquad (2)$$

In equation (2), P_c and E_c are terms characterizing the interactions of the atoms at $T = 0°K$; $P_{t.l}$ and $E_{t.l}$ are thermal terms due to the vibration of the atomic lattice; $P_{t.e}$ and $E_{t.e}$ are the terms due to the thermal excitation of the electrons. The necessity for taking the electronic terms into account is due to the fact that, in the regions of temperature and pressure which we are considering, their contribution is already important, as will become evident from what follows later.

Let us consider the individual terms in (2). It has been shown that the function $P_c(v)$, and consequently also $E_c = \int_v^{v_{0k}} P_c\,dv$, must be found from experimental measurements (v_{0k} is the specific volume at $P = 0$ and $T = 0°K$). We shall write the thermal terms for the lattice, in conformity with the conclusions of solid state theory, in the form

$$E_{\text{t.l.}} = C_{vl}\left(T - T_0 + \frac{E_0}{C_{vl}}\right) \qquad (3a)$$

$$P_{\text{t.l.}} = \gamma_l(v)\frac{C_{vl}}{v}\left(T - T_0 + \frac{E_0}{C_{vl}}\right). \qquad (3b)$$

TABLE III

U, km/sec	D, km/sec				U, km/sec	D, km/sec			
	Aluminum	Copper	Lead	Iron		Aluminum	Copper	Lead	Iron
0	5.20	3,92	1.91	—	3.5	10.41	9,19	7.00	9.54
0,5	5.94	4.68	2.75	—	4.0	10.81	9,93	7,59	10,33
1.0	6.64	5.44	3.56	5,38	4,5	11.48	10.67	8,18	11,10
1.5	7.32	6.22	4.33	6.30	5.0	12.16	—	—	—
2.0	8.02	6,96	5.07	7,15	5.5	12.82	—	—	—
2,5	8,71	7.70	5.75	7.96	6,0	13.45	—	—	
3.0	9.41	8,45	6.38	8.76					

TABLE IV

	Aluminum	Copper	Lead		Aluminum	Copper	Lead
ρ_0, g/cm^3	2.71	8.93	11.34	$(d\ln\gamma_l/d\ln v)_{v_0}$	1.175	1.265	1.400
C_{vl}, 10^6 erg/g-deg	8,960	3.825	1.293	m	3.5	4.3	5.0
E_0, 10^7 erg/g	161.0	77,1	32,3	n	6,0	6.0	7.0
$\varkappa_0$, 10^{-12} cm^2/d	1.367	0.730	2.415	β_0, erg/g-deg^2	500	110	144
α, 10^{-6} deg^{-1}	23.1	16.5	29.0	v_{0k}/v_0	0.988	0,990	0.979
γ_0	2.088	1.983	2.457	$-v_0(dP_c/dv)_{v_{0k}}$, $10^{10}\frac{\text{d}}{\text{cm}^2}$	77.10	142.82	45.89

Here C_{vl} is the specific heat of the lattice; E_0 is the internal energy under normal conditions; $\gamma_l(v)$ is the Grüneisen coefficient for the lattice, which is a function of the specific volume; and v is the specific volume.

In Eq. (3) it is assumed that the specific heat is independent of the temperature and density, as a consequence of which the Grüneisen coefficient also becomes independent of the temperature. The assumption of constant C_{vl} is, of course, an approximation which does not take into account the anharmonicity of the vibrations in the solid.

Solid state theory provides a connection between the Grüneisen coefficients and the derivatives of the curve $P_c(v)$. According to Slater[1] and Landau[2]

$$\gamma_l(v) = -\frac{v}{2}\left[\frac{d^2P_c/dv^2}{dP_c/dv}\right] - \frac{2}{3}. \tag{4a}$$

According to Dugdale and MacDonald[3]

$$\gamma_l(v) = -\frac{v}{2}\left[\frac{d^2(Pv^{2/3})/dv^2}{d(Pv^{2/3})/dv}\right] - \frac{1}{3}. \tag{4b}$$

Let us consider the limits of variation of $\gamma_l(v)$.

Under normal conditions, by definition

$$\gamma_0 = \gamma_l(v_0) = -\frac{v_0^2}{C_{vp}}\left(\frac{\partial P}{\partial v}\right)_{T=T_0}\frac{1}{v_0}\left(\frac{\partial v}{\partial T}\right)_{P=0} = \frac{3\alpha}{\rho_0 C_{v_l}\varkappa_0}, \tag{5}$$

where α is the coefficient of linear thermal expansion; κ_0 is the coefficient of volume compressibility for $P = 0$ and $T = T_0$; and $v_0 = 1/\rho_0$ is the specific volume under normal conditions. The values of the parameters E_0, ρ_0, C_{vl}, α, κ_0, and γ_0 for aluminum, copper, and lead are given on the left hand side of Table IV. For these metals the initial values γ_0 are close to 2, and are all included within a rather narrow range of values.

Some idea of the behavior of the function $\gamma_l(v)$, for v close to v_0, can be obtained by substituting the expression for $P_c(v)$ resulting from the Mie-Lennard-Jones potential[10] into the relation (4a) or (4b). Using formula (4b),

$$\gamma_l(v_0) = \tfrac{1}{6}(n + m + 3), \tag{6}$$

$$(d\ln\gamma_l/d\ln v)_{v_0} = (n+2)(m+2)/18. \tag{7}$$

The quantities $(d\ln\gamma_l/d\ln v)_{v_0}$ from (7) are given in Table IV. The exponents m and n used

TABLE V. Aluminum

ρ/ρ_0	P_c, 10^{10}d/cm^2	E_c, 10^8 erg/g	P_Γ, 10^{10} d/cm^2	T, °K	γ_l	ρ/ρ_0	P_c, 10^{10}d/cm^2	E_c, 10^8 erg/g	P_Γ, 10^{10} d/cm^2	T, °K	γ_l
1,05	3,1	2,0	4,2	315	2,00	1,45	61.9	249.0	71.3	1980	1.41
1.10	7,8	10.5	9.0	348	1.81	1.50	72.7	306.0	86.1	2640	1.44
1.15	13,4	26.0	14.5	401	1.56	1.55	84.5	368.0	103.0	3440	1.44
1.20	19,7	47.0	21,1	488	1.37	1.60	97.0	435.0	121,7	4410	1.43
1.25	26,6	76.0	28.8	625	1.28	1.65	110.0	508.0	142.7	5530	1.41
1,30	34.5	111,0	37,4	818	1,28	1.70	125,0	585,0	165.2	6790	1.39
1,35	42,9	151.0	47,2	1097	1.31	1.75	140.0	667.0	189.7	8180	1,34
1,40	51,9	198,0	58.2	1476	1,37	1.80	157,0	754.0	216.0	9670	1.30

TABLE VI. Copper

ρ/ρ_0	P_c, 10^{10}d/cm²	E_c, 10^8 erg/g	P_Γ, 10^{10} d/cm²	T, °K	γ_l	ρ/ρ_0	P_c, 10^{10}d/cm²	E_c, 10^8 erg/g	P_Γ, 10^{10} d/cm²	T, °K	γ_l
1.05	6,1	1.3	7.5	317	1.89	1,40	105.2	117.0	122.5	2300	1.63
1.10	15,1	6.3	46.7	360	1.85	1.45	127.2	148.7	152.2	3180	1.59
1.15	25.4	15.1	28.0	438	1.87	1.50	151.8	184.8	185.8	4350	1.55
1.20	37.5	27.9	41,3	577	1.88	1.55	178.3	224.0	225.2	5760	1.53
1.25	51.6	44.6	56.6	802	1,84	1,60	207.5	267.2	271.4	7530	1.53
1.30	67.4	64.7	75.5	1150	1,77	1.65	238,7	314.5	324.7	9710	1.53
1.35	85.3	89.1	97.1	1630	1.70	1.70	273.0	366.0	388.0	12425	1.54

in equation (7) are shown in the same place.* The sign and absolute magnitude of $(d \ln \gamma_l / d \ln v)_{v_0}$ show that the Grüneisen coefficient increases rapidly with a decrease in the specific volume. From Gilvarry's data,[11] as the pressure increases without limit, γ_l tends to a limiting value of $\frac{2}{3}$.

The electronic heat terms in the energy and pressure are proportional to the square of the temperature for a degenerate electron gas. This conclusion follows not only from free electron theory, but also from the solution of the Thomas-Fermi equations obtained by Gilvarry.[12] By making use of the concept of an electronic specific-heat coefficient β, they can be rewritten in the form

$$E_{t.e.} = \tfrac{1}{2}\beta T^2, \quad P_{t.e.} = \gamma_e E_{t.e.}/v = \tfrac{1}{2}\gamma_e \beta T^2/v. \tag{8}$$

Here γ_e is a coefficient defined as the ratio of the electrons' thermal pressure to their thermal energy.

A comparison of Latter's data,[13] giving an accurate solution of the Thomas-Fermi equation for the case $T \neq 0$, with Gilvarry's data for the case $T \approx 0$ shows that the electronic specific heat coefficient remains almost constant up to temperatures of the order of 30 to 50 × 10³ °K. Furthermore, as the density increases, this constancy is maintained up to higher temperatures. In order to explain the dependence of the electronic specific heat coefficient on the degree of compression, we make use of the thermodynamic identity

$$(\partial E/\partial v)_T = T(\partial P/\partial T)_v - P.$$

Substituting $E_{t.e}$ and $P_{t.e}$ from (8) into this expression we obtain, after integration,

$$\beta = \beta_0 \exp\left\{\int_{v_0}^{v} \gamma_e \frac{dv}{v}\right\}.$$

An analysis of the data of Gilvarry and Latter shows that the magnitude of the Grüneisen coefficient for electrons, γ_e, varies within the rather narrow limits 0.5 to 0.6, tending at extremely high pressures to the value $\frac{2}{3}$, characteristic of a free electron gas. If we take $\gamma_e = \frac{1}{2}$ over the region of interest to us, we obtain $\beta = \beta_0 (v/v_0)^{1/2}$ and accordingly

$$E_{t.e.} = \tfrac{1}{2}\beta_0 (v/v_0)^{1/2} T^2; \quad P_{t.e.} = \tfrac{1}{4}\beta_0\rho_0 (v_0/v)^{1/2} T^2. \tag{9}$$

The value of β_0 may be taken from experimental measurements at low temperatures. It is well known that the electronic specific heat, which under normal conditions is an extremely small fraction of the lattice specific heat (~ 3%), becomes noticeable at temperatures close to the absolute zero, because in this region the specific heat due to lattice vibrations drops off as T^3, while the specific heat of the electron gas is proportional to T. The values of the experimentally determined electronic specific heat coefficients β_0, used in the calculations below, are given in Table IV.

Adding the terms P_c and E_c to the electronic and lattice thermal terms, we obtain the following expressions for the pressure and energy:

$$P = P_c + \frac{\gamma_l C_{vl}}{v}[T - T_0 + E_0/C_{vl}] + \tfrac{1}{4}\rho_0\beta_0 (v_0/v)^{1/2} T^2; \tag{10a}$$

$$E = \int_{v}^{v_{0k}} P_c \, dv + E_0 + C_{vl}(T - T_0) + \tfrac{1}{2}\beta_0 (v/v_0)^{1/2} T^2. \tag{10b}$$

Let us now, following Walsh,[5] establish a connection between the parameters of the metal in its initial state and the coefficients a_k of the dynamic adiabats. In order to obtain the necessary relations, we recall that the isentropic curve which passes through the origin of coordinates has a second-order tangency with the Hugoniot adiabat. Its coefficients, when expressed in a series analogous to (1),

$$P_s = \sum_k a_k(s)(\sigma - 1)^k,$$

are connected with the coefficients of the Hugoniot adiabat by the expressions:

$$a_1(s) = a_1; \quad a_2(s) = a_2;$$
$$a_3(s) = a_3 - \tfrac{1}{6}\gamma_0(a_1 + a_2). \tag{11}$$

The first coefficient $a_1(s)$ is the isentropic modulus of bulk compression, i.e., the reciprocal of the compressibility coefficient κ. For all prac-

---

*m and n have been chosen from the experimental values of the sublimation energies and the coefficients $\gamma_l(v_0)$.

tical purposes it does not differ from the isothermal modulus measured by Bridgman.[14]

Substituting P_S into (4a) and then differentiating leads to the equation

$$a_2(s) = a_1(s)\,\gamma_0;$$

$$\gamma_0\left(\frac{d\ln\gamma}{d\ln v}\right)_{v=v_0} = 2\left(\frac{a_2(s)}{a_1(s)}\right)^2 - \frac{10}{6}\left(\frac{a_2(s)}{a_1(s)}\right) - 3\frac{a_3(s)}{a_1(s)} - \frac{1}{9}.$$

In view of (11), we obtain finally

$$a_1 = \frac{1}{\varkappa_0};\quad a_2 = \frac{\gamma_0}{\varkappa_0};$$

$$a_3 = \frac{a_1}{3}\left[\frac{5}{2}\left(\frac{a_2}{a_1}\right)^2 - \frac{7}{6}\left(\frac{a_2}{a_1}\right) - \gamma_0\left(\frac{d\ln\gamma}{d\ln v}\right)_{v_0} - \frac{1}{9}\right]. \quad (12)$$

In calculating the coefficients a_1, a_2, and a_3, the values of κ_0, γ_0, and $(d\ln\gamma_l/d\ln v)_{v_0}$ were taken from Table IV.

3. RESULTS OF THE CALCULATIONS

The results of dynamic experiments, expressed in the form (1), determine the pressure P_Γ, and also the energy $E_\Gamma = E_0 + \frac{1}{2}P_\Gamma(v_0 - v)$. Substituting these quantities into the left hand side of (10a) and (10b) gives us two equations, containing three unknown functions P_c, γ_l, and T. The missing third equation is (4b). The initial conditions of the system will be

$$P_c(v_{0k}) = 0 \text{ and } (dP_c/dv)_{v_{0k}}.$$

The method of calculating v_{0k} and $(dP_c/dv)_{v_{0k}}$ is given in Walsh's paper,[5] and the values of these quantities which have been used in the calculations are given in Table IV.

The results of the numerical solution of the system for aluminum, copper, and lead are given in Tables V to VII, respectively. In these tables are given the pressures and compressional energies at the absolute zero of temperature, the pressures and temperatures of the Hugoniot adiabat, and the values of the Grüneisen coefficient.

The relative positions of the Hugoniot adiabats and the curves of "cold" compression are demonstrated in Figs. 1 and 2. As the figures show, thermal pressure plays an important role in the compression of metals by strong shock waves. Thus, for pressures of 216×10^{10} d/cm^2 in aluminum, 388×10^{10} d/cm^2 in copper, and 401×10^{10} d/cm^2 in lead, the thermal components of the pressure are equal to 59×10^{10}, 115×10^{10}, and 124×10^{10} d/cm^2, respectively.

The role of the heat in the internal energy balance is even larger. In this case, for the same compressive shock pressures as above, the thermal energy has become the major fraction, amounting to 57% for aluminum, 60% for copper, and 69% for lead.

The temperatures attained were 9700, 12,400, and 26,200 degrees, which are approximately twice as high as the melting points of the metals, as estimated for the high pressure region by Gilvarry.[11] High temperatures lead to a considerable increase in the specific heat of the metal, due to its electronic component βT. There is a corresponding increase in the contribution of the electrons to the internal energy balance. For example, in the shock compression of lead to $\rho = 2.2\rho_0$ the electronic fraction of the thermal energy amounts to about 34% of the total internal energy change, and to 50% of its thermal part. The corresponding proportions of the thermal pressure due to the electrons are 10% and 34%.

As expected, in all three metals a general tendency was observed for $\gamma_l(v)$ to decrease with density. It should be noted that the value of the function $\gamma_l(v)$ depends markedly on small variations in the positions of the dynamic adiabatics. On the other hand, the shape of the cold compression curves is much less sensitive to possible variations in the dynamic adiabatics, especially in the region of large thermal pressures. The positions of the P_c curves also change very little when the expression (4b) for γ_l is substituted for the Landau-Slater formula (4a), or when the quantity β_0 is varied.

TABLE VII. Lead

ρ/ρ_0	P_c, 10^{10}d/cm^2	E_c, 10^8 erg/g	P_Γ, 10^{10} d/cm^2	T, °K	γ_l	ρ/ρ_0	P_c, 10^{10}d/cm^2	E_c, 10^8 erg/g	P_Γ, 10^{10} d/cm^2	T, °K	γ_l
1.10	4.2	1.2	5.3	364	2.20	1.80	123.7	127.3	176.5	11590	1.48
1.20	11.6	6.2	13.4	563	2.00	1.85	139.5	144.6	200.7	13260	1.42
1.30	21.6	15.3	25.0	1045	1.90	1.90	156.0	163.2	225.5	15000	1.35
1.40	34.6	28.8	42.3	2000	1.84	1.95	173.8	182.8	251.2	16720	1.28
1.50	51.0	46.7	65.5	3550	1.77	2.00	192.6	203.5	277.6	18470	1.21
1.55	60.7	57.2	79.7	4570	1.73	2.05	212.3	225.2	305.5	20300	1.14
1.60	71.3	69.0	95.5	5730	1.69	2.10	233.0	248.2	335.5	22150	1.07
1.65	82.7	81.7	113.5	7070	1.65	2.15	254.5	272.0	367.7	24125	1.02
1.70	95.3	95.8	133.0	8485	1.60	2.20	277.0	297.0	401.0	26230	0.98
1.75	109.2	111.1	154.0	10000	1.54						

The shape of the curves $P_c(v)$ is also apparent from the results of the present work.

The authors express their thanks to A. I. Funtikov for valuable discussions and participation in the series of experiments, and also to R. V. Malyshev and I. P. Dudoladov for the large volume of computational work which they accomplished. With especial gratitude the authors acknowledge the valuable consultations with Prof. K. A. Semendyaev.

---

[1] J. C. Slater, Introduction to Chemical Physics, McGraw, New York (1939).

[2] L. D. Landau and K. P. Stanyukovich, Dokl. Akad. Nauk SSSR **46**, 399 (1945).

[3] J. S. Dugdale and D. K. MacDonald, Phys. Rev. **89**, 832 (1953).

[4] Al'tshuler, Krupnikov, Lebedev, Zhuchikhin, and Brazhnik, JETP **34**, 874 (1958), Soviet Phys. JETP **7**, 606 (1958).

[5] Walsh, Rice, McQueen, and Yarger, Phys. Rev. **108**, 196 (1957).

[6] Al'tshuler, Krupnikov, and Brazhnik, JETP **34**, 886 (1958), Soviet Phys. JETP **7**, 614 (1958).

[7] J. M. Walsh and M. H. Rice, J. Chem. Phys. **26**, 815 (1957).

[8] H. D. Mallory, J. Appl. Phys. **26**, 555 (1955).

[9] Bancroft, Peterson, and Minshall, J. Appl. Phys. **27**, 291 (1956).

[10] E. Grüneisen, Handbuch der Physik, Springer, Berlin, (1926), vol. 10, p. 1.

[11] J. J. Gilvarry, Phys. Rev. **102**, 317 (1956).

[12] J. J. Gilvarry, Phys. Rev. **96**, 934, 944 (1954); J. J. Gilvarry and G. H. Peebles, Phys. Rev. **99**, 550 (1955).

[13] R. Latter, Phys. Rev. **99**, 1854 (1955).

[14] P. V. Bridgman, The Physics of High Pressure, Bell (1949); Recent Work in the Field of High Pressures, Revs. Modern Phys. **18**, 1 (1946).

Translated by D. C. West
155